Nozzle Wall Boundary Layers at Mach Numbers 20 to 47

JOSEPH H. KEMP JR.* AND F. K. OWEN †
NASA Ames Research Center, Moffett Field, Calif.

The nozzle wall boundary layer of the Ames M-50 helium tunnel has been thoroughly investigated with Pitot pressure, total temperature, skin friction, wall heat transfer and hot wire measurements at 5 stations. A flow model suggested by the results is presented and discussed. Hot wire measurements indicate pronounced intermittency at the outer edge of the boundary layer. The direct skin-friction measurements are higher than expected from empirical predictions and the Reynolds analogy factor, $2C_H/C_f$, is less than unity.

Nomenclature

C_f = friction coefficient
C_H = heat-transfer coefficient, $q/\rho_e u_e C_p(T_{aw}-T_w)$
d = diameter of thermocouple wire used in heat-transfer gage
D = diameter of wire in total temperature probe
e = voltage
f = frequency
F_c = transformation function for C_f
F_{R_θ} = transformation function for Re_θ
h = heat-transfer coefficient, $q/(T_{aw}-T_w)$
k = thermal conductivity
M = Mach number
Nu = Nusselt number
p = pressure
q = wall heat-transfer rate
Q_R = total heat conduction at radius R in the thin skin at the heat-transfer gage
R = radius
R_θ = Reynolds number based on momentum thickness
t = thickness of sensing element in heat-transfer gage
T = temperature
u = velocity
u^+ = transformed velocity
y = distance normal to the surface
y^+ = transformed distance normal to the surface
δ = boundary-layer thickness
θ = momentum thickness
μ = coefficient of viscosity
ν = kinematic viscosity
ρ = density
τ = shear stress

Subscripts

act = actual value
c = at disk center
e = outer edge of the boundary layer
L = outer edge of the viscous sublayer
m = measured value
R = at radius R
VD.I = Van Driest I
w = wall or wire
o = local stagnation condition
2 = static value behind a normal shock

Introduction

PREDICTION of skin friction and heat transfer on hypersonic flight vehicles requires an increased understanding of hypersonic turbulent boundary layers. This understanding requires experimental data over the full range of possible flight conditions to aid in the development of flow models and to provide test cases for various proposed theories and prediction techniques. At the present time, published data for Mach numbers above 15 are somewhat limited; however, they indicate that significant differences exist between hypersonic boundary layers and those in the subsonic and supersonic range. Data presented in Ref. 1 indicate that in high Mach number low-density flows, turbulent boundary layers may have substantially thicker viscous sublayers and the significant pressure gradients may exist normal to the wall. In regard to the latter effect, Fischer et al.[2] recently correlated normal pressure gradient effects with Mach number for many facilities and showed further that similar pressure gradients exist in turbulent boundary layers on cones, wedges, and flat plates. They also found much larger mass flow fluctuations than previously observed at lower Mach numbers, in hypersonic turbulent boundary layers and that these fluctuations reach a maximum somewhere near the wall, probably at or near the outer edge of the viscous sublayer.

This paper extends previous work[1] on hypersonic nozzle boundary layers. It presents results of direct measurements of skin friction and wall heat-transfer rates along with mean and fluctuating measurements across the nozzle wall boundary layer in the Ames M-50 helium tunnel.

Experiment

Test Facility

The Ames M-50 helium tunnel,[3] a blowdown tunnel with an axisymmetric contoured nozzle and an open test section, uses heated helium as a test gas and operates at nominal exit Mach numbers of 42 for test times up to 20 min. The 3.61 M-long nozzle has an exit radius of 0.356 M.

Figure 1 shows the five survey stations where Pitot pressure, total temperature, and wall temperature were measured, together with the 10 wall pressure stations. Wall heat transfer and skin friction were also measured at the last 4 survey stations. Hot-wire surveys were made at the last two stations. The tunnel was operated at reservoir pressures ranging from 65 to 272 atm and total temperatures from 300° to 880°K.

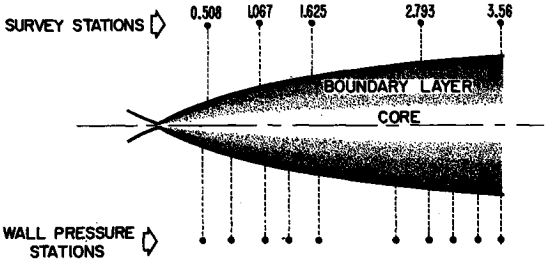

Fig. 1 Schematic drawing of the M-50 nozzle.

Presented as Paper 71-161 at the AIAA 9th Aerospace Sciences Meeting, New York, January 25–27, 1971; submitted February 18, 1971; revision received March 2, 1972.

Index categories: Boundary Layers and Convective Heat Transfer; Supersonic and Hypersonic Flow; Nozzle and Channel Flow.

* Research Scientist.
† Postdoctoral Research Associate.

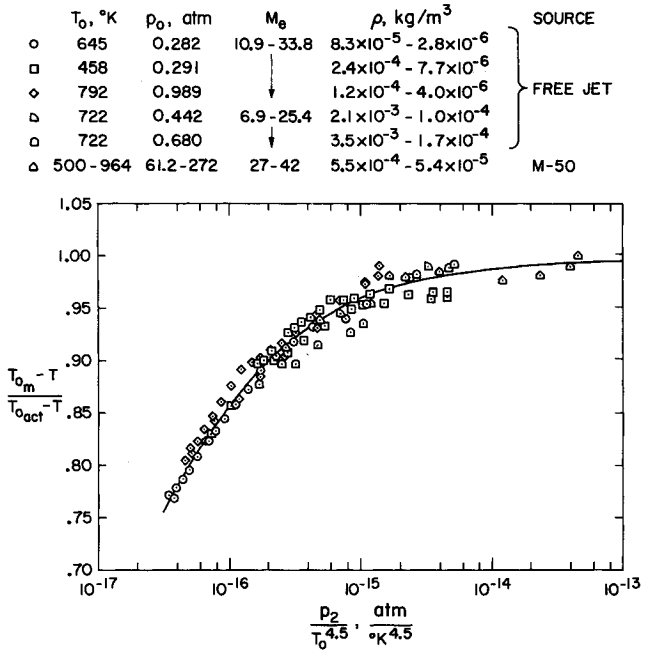

Fig. 2 Correlation of calibration data for the total temperature probe.

Pressure Measurements

Pitot pressure surveys were made by traversing a single 0.475 cm-diam probe through the boundary layer. Pressures were measured by a modular pressure transducer system similar to one described in Ref. 4. This system uses a capacitance type transducer that measures differential pressures, and one transducer provides accurate readings over the full pressure range (0.0004–0.14 atm) encountered in the boundary layer. Errors in pressure resulting from nonlinearity and temperature effects on the transducer sensitivity were less than $\pm 1\%$ of the measured value. Additional errors due to variations in reference pressures are less than 4% of the minimum pressure measured.

No corrections were made for the various rarefaction effects on the pressure measurements. However, the possible variations from these effects are summarized as follows. The effects of thermal transpiration errors due to temperature variations along the tube connecting the orifice and the transducer are negligible.[5,6] Errors in wall pressure resulting from orifice effects due to heat transfer to the wall are less than 3%.[7] Errors due to viscous interaction and rarefaction effects on the Pitot pressure measurements are less than 4% for the outer region of the boundary layer.[8] Near the wall, within 20%–40% of the boundary-layer thickness, these effects may introduce much larger errors; however, they should not influence the conclusions drawn from the data.

Stagnation Temperature Measurements

Stagnation temperatures were measured with a single shielded, 0.178 cm-diam thermocouple probe designed for use under very low-density flow conditions. This probe consists of a fine wire, butt-welded chromel-alumel thermocouple, with an over-all length-to-diameter ratio of 200 suspended between needle-like supports and enclosed in radiation shield.

The probe was calibrated in the free-jet facility described in Ref. 9 which produced flows at Mach numbers ranging from 5 to 40 at densities comparable to those encountered in the boundary layer of the M-50 tunnel. A few check points were also made in the freestream of the M-50 tunnel. The calibration data are correlated over a wide range of temperatures and pressures in Fig. 2. These data could not be correlated solely on the basis of conduction error as proposed by Winkler.[10] The present correlation parameters were derived assuming that radiation losses constituted the major source of error (see Appendix). Conduction effects probably cause some scatter in the data. However, in spite of this, the correlation is reasonably good for a wide range of temperatures and there is substantial agreement between the calibration in the freejet and the test points in the M-50.

Skin-Friction Measurements

Skin friction was measured using a floating element, magnetically nulling balance similar to the one described in Ref. 11. At each station, the elements were contoured to the local nozzle surface. The balance had a reading error less than 1% of the minimum measured skin friction. Investigation of the effects of floating element position, both above and below the surface, showed that the measured skin friction was much less sensitive to the element position than has been observed previously at lower Mach numbers[12–14] probably due to the relatively large thickness of the boundary layer. Indeed, the indicated skin friction increased by only 10% when the element was raised 0.0075 cm above the surface.

Heat-Transfer Measurements

Wall heat transfer was determined from the steady-state heat conduction in a thin-skin gage contoured to the nozzle wall. To accomplish this local temperatures were measured by means of chromel-constantan thermocouples spot-welded to the thin skin at the location shown in Fig. 3. Since the temperature variation between the center of the disk and the wall was small, relative to the driving potential, constant heat transfer over the gage surface area was assumed. With this assumption, the equation governing the heat transfer in the gage is

$$Q_R = -2\pi Rkt(dT/dR) = -\pi R^2 q$$

Solving for the temperature, one obtains

$$q = [(T_c - T_R)/R^2]4tk$$

In the present experiments, heat-transfer rates corresponding to the temperature difference between the center and each of the other three thermocouples (see Fig. 3) were calculated and the results averaged to obtain the values presented here.

Errors due to conduction down the thermocouple wires, convection from the back of the gage, and radiation losses were neglected. Estimates indicate less than 5% combined error due to these effects. Additionally, basic instrument accuracy and the accuracy of normalizing quantities (ρ, u, T_{aw} and T_w) also introduce error in the heat-transfer coefficient. Consequently the over-all accuracy of the heat-transfer coefficient is estimated to be about $\pm 12\%$.

Boundary-Layer Fluctuation Measurements

The character of the fluctuations across the boundary layer were obtained with a constant temperature anemometer system with a water-cooled platinum film probe similar to the one described in Ref. 15. Water cooling enabled the film to be operated at a temperature well below the freestream total temperature. The upper frequency limit (−3 db) of the system, as determined by a standard square-wave technique, was 60 kHz. Since the boundary layer is approximately 29 cm thick at the survey station this frequency response makes it possible to measure fluctuations with a length scale down to one-eighth the

STATION, x, m	SKIN THICKNESS, t, cm	THERMOCOUPLE WIRE DIAMETER, d, cm
1.067	0.0152	0.0075
1.625	0.0127	0.0075
2.793	0.0076	0.0025
3.56	0.0051	0.0025

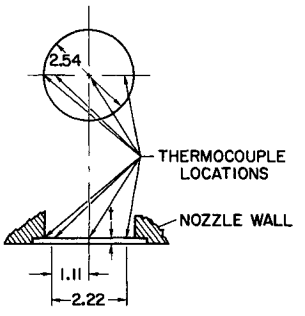

Fig. 3 Schematic of the heat-transfer gage.

Table 1 Test parameters

X	M_e	P_o	T_o	δ	$P_w \times 10^4$	T_w	$C_f \times 10^4$	C_H	$\rho_w \times 10^5$	δ_L/δ	U_L/U_e	M_L/M_e	R_θ
0.508	19.4	66.1	499	2.87	5.26	362	4.87[a]		7.1	0.3	0.95	0.24	1381
	19.2	66.2	820	2.87	5.26	397	4.84[a]		6.54	0.39	0.94	0.28	913
	19.9	107.6	315	2.72	8.61	333	4.06[a]		12.55	0.19	0.94	0.16	2662
	19.9	107.6	393	2.74	8.61	333	4.28[a]		12.65	0.20	0.93	0.16	2608
	19.8	108.1	481	2.72	8.61	339	3.78[a]		12.43	0.25	0.94	0.13	2196
	19.8	109.2	988	2.69	8.61	400	4.38[a]		10.67	0.29	0.91	0.18	1420
	20.1	199	516	2.44	13.4	352	3.37[a]		18.73	0.17	0.90	0.09	3343
	20.0	199	942	2.57	13.4	409	3.71[a]		16.40	0.28	0.88	0.18	2688
	20.3	270	503	2.36	18.1	318	2.39[a]		27.9	0.18	0.92	0.18	5430
	20.2	268	882	2.41	18.2	361	3.42[a]		24.8	0.21	0.91	0.21	3337
1.067	27.3	65.3	500	7.98	1.45	315	3.62	1.21	2.23	0.39	0.93	0.20	1440
	26.4	65	933	7.67	1.45	358	3.94	1.41	1.98	0.46	0.93	0.22	916
	27.3	107.7	305	7.11	2.08	299	2.33	0.866	3.37	0.25	0.94	0.18	3786
	27.5	107.7	418	7.11	2.08	301	2.53	0.967	3.39	0.31	0.94	0.18	2767
	27.9	107.7	577	7.16	2.08	309	3.02	1.16	3.30	0.33	0.92	0.17	1801
	27.4	109.8	920	7.24	2.04	328	3.22	1.22	3.04	0.38	0.92	0.19	1685
	29.4	189	534	6.96	3.12	319	2.73	1.11	4.78	0.28	0.94	0.18	3710
	29.0	189	877	6.99	3.12	348	3.01	1.02	4.36	0.32	0.93	0.17	2380
	29.9	270	502	6.47	3.86	318	2.03	0.957	5.89	0.23	0.93	0.15	4756
	29.6	265	876	6.60	3.85	339	2.58	1.02	5.35	0.29	0.92	0.16	2870
1.625	30.9	66.9	515	13.34	0.698	301	2.66	0.758	1.14	0.40	0.94	0.20	2190
	30.6	65.3	890	13.46	0.698	321	3.00	1.00	1.085	0.46	0.94	0.21	1296
	33.1	107.3	495	12.57	1.05	306	2.38	0.797	1.72	0.36	0.93	0.14	2800
	32.5	107.6	886	12.70	1.04	317	2.72	0.931	1.634	0.42	0.93	0.18	1680
	34.5	198	515	11.42	1.45	304	1.96	0.679	2.32	0.31	0.93	0.14	4096
	34.9	200	888	11.68	1.45	321	2.45	0.920	2.24	0.35	0.93	0.15	2916
	35.8	268	514	11.04	1.88	302	1.88	0.794	3.06	0.26	0.92	0.12	5582
	35.1	263	893	11.17	1.87	314	2.17	0.782	2.97	0.34	0.92	0.17	3378
2.793	38.1	108.2	523	25	0.395	300	1.64	0.493	0.658	0.40	0.94	0.14	2074
	37.9	110.2	967	24.1	0.395	300	1.90	0.680	0.640	0.46	0.94	0.25	1450
	42.2	200	498	21.3	0.553	300	1.47	0.418	0.902	0.35	0.92	0.09	3308
	42.1	201	958	21.8	0.553	300	1.79	0.576	0.925	0.41	0.94	0.12	1645
	44.6	270	523	21.3	0.658	300	1.44	0.501	1.103	0.33	0.94	0.13	4412
	43.5	271	913	21.6	0.658	300	1.65	0.666	1.092	0.38	0.94	0.12	2330

* These values estimated from velocity profiles.

boundary-layer thickness, i.e., $f\delta/U_\infty = 8$. In light of the work by Kistler,[16] such a length scale should be adequate.

Mass flow and temperature fluctuation intensities were also measured across the boundary layer using a 0.00063-cm-diam by 0.317-cm-long platinum 10% iridium wire. A preliminary calibration of the wire made in the freejet facility[9] showed that $(\partial e^2/\partial T_o)_{\rho u, T_w}$ and $(\partial e^2/\partial \rho u)_{T_o, T_w}$ were approximately constant over the range of test conditions. This is consistent with the indication that for this diameter wire the flow should be essentially free molecular. Mass flow and total temperature fluctuation levels were obtained at a number of points through the boundary layer using a technique similar to that of Kistler.[16] The wire was operated at 6 different overheat ratios and a least squares parabolic fit of the data was made to the equation

$$\Delta e^2 = \left(\frac{\partial e}{\partial T_o}\right)^2 \overline{(\Delta T_o)^2} + \left(\frac{\partial e}{\partial \rho u}\right)^2 \overline{(\Delta \rho u)^2} + 2\frac{\partial e}{\partial \rho u}\frac{\partial e}{\partial T_o}\overline{\Delta \rho u T_o}$$

where $\partial e/\partial T_o$ and $\partial e/\partial \rho u$ were obtained from the calibration.

Results and Discussion

The present test conditions provide Reynolds numbers based on throat diameter ranging from 0.5×10^6 to 4.8×10^6. Consequently, considering the data given in Ref. 17, the boundary layer is probably turbulent at the throat even though large favorable pressure gradients may tend to stabilize it. The possibility of relaminarization due to the favorable pressure gradient has been examined and using the parameter of Back et al.[18] it appears that some relaminarization might be expected for the lower pressure test conditions in a region about 1 cm long just ahead of the throat. For the highest pressure conditions no relaminarization is predicted. Thus, it appears unlikely that relaminarization due to pressure gradient is a major factor in the flow.

It is possible that nonequilibrium or history effects as discussed in Refs. 19 and 20 exist in the present flow however no definitive information regarding these effects for this flow are available at the present time.

A summary of various parameters associated with the data is presented in Table 1. The data for station 3.56 are not presented because of interference effects at the end of the nozzle ($x = 3.61$ m).

Velocity and density profiles were calculated using faired values from the measured Pitot pressure and stagnation temperature profiles. In obtaining these velocity and density profiles the static pressure was assumed to vary linearly through the boundary layer as $p = p_w + (p_e - p_w)(y/\delta)$; an example of the resulting profile is shown in Fig. 4. Also presented in this figure are values obtained with the assumptions $p = p_w$ and $p = p_e$. As can be seen variations in p make little difference in the outer region of the boundary layer. However, in the inner region "$p = p_e$" provides substantially different values than do the other two assumptions. It is unlikely that large pressure gradients in the y direction could exist near the wall since both Mach number and density are low in this area. Consequently "$p = p_e$" is probably the least accurate assumption in this area. Although the other two assumptions given nearly identical profiles, the linear variation is used for the present work because it matches the true conditions at the outer edge of the boundary layer. This assumption is not exact, however, barring any large excursions in p—values much larger than p_w or much smaller than p_e—this assumption should not substantially affect the conclusions of this paper.

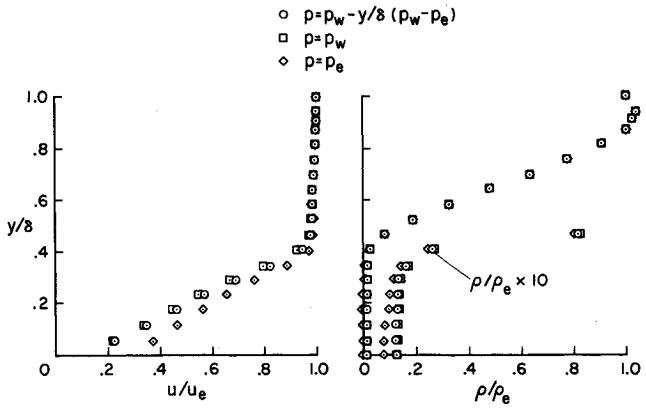

Fig. 4 Typical velocity and density profiles $M = 42.1$, sta = 2.793 m.

The general nature of the velocity and density profile was discussed in Ref. 1 where it was pointed out that the boundary layer has a relatively thick inner region with linear velocity variations typical of those occurring in a viscous sublayer and an outer region with small velocity and large density variations typical of profiles normally associated with a turbulent boundary layer. The skin-friction measurements suggest a velocity slope at the wall which is in excellent agreement with the measured velocity profile.

The improved accuracy in the total temperature measurements of the present experiments reveals that the density is nearly constant across the viscous sublayer and that a density overshoot exists near the outer edge of the boundary layer. The density overshoot was not observed during the previous investigation (Ref. 1) because the boundary-layer edge was assumed to be at the peak Pitot pressure location. However the present temperature measurements indicate the existence of velocity gradients further from the wall, thus making it necessary to redefine the edge of the boundary layer. The point chosen for the present tests is where local total temperatures first deviate from the reservoir temperature. This density overshoot may be explained by the fact that the data were obtained on a hypersonic nozzle wall forward of the point where the flow is fully expanded. Thus, the inviscid density variation is similar to that shown schematically in Fig. 5 (see Ref. 3). Interaction of this variation with the wall boundary layer would result in density variations similar to those shown by the dashed line.

Effects of Wall Temperature Ratio

Total temperature variations across the boundary layer are shown in Fig. 6 for various wall temperature ratios T_w/T_{o_e} obtained by varying the freestream total temperature. These surveys were obtained at the 1.067 meter station where the edge Mach number was sufficiently low that wall temperature ratios near unity could be obtained without liquefaction problems.

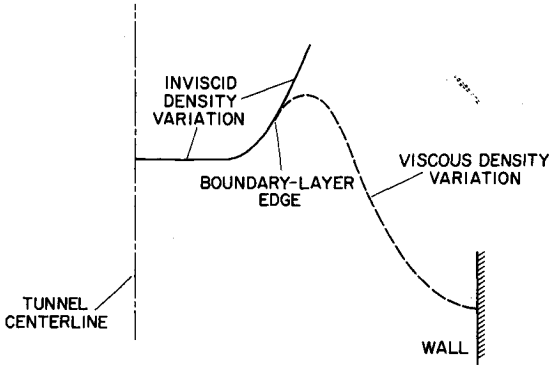

Fig. 5 Schematic of coupling between the inviscid and viscous density variations.

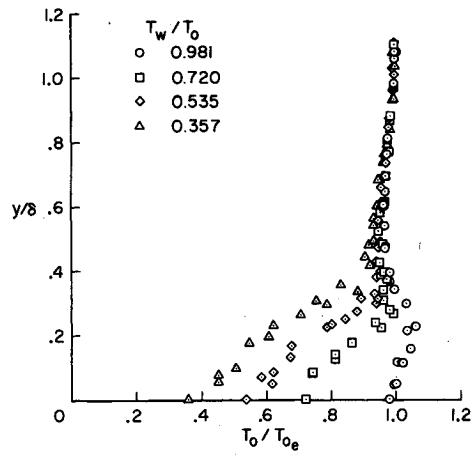

Fig. 6 Variation in temperature profiles with wall temperature ratio; $M_e \approx 27$, sta = 1.067 m.

For $T_w/T_{o_e} = 0.98$ an overshoot in the total temperature occurs near the outer edge of the viscous sublayer ($y/\delta \approx 0.2$). Further from the wall the temperature drops to a value lower than T_w($y/\delta \approx 0.4$) and then rises uniformly to T_{o_e} at the edge of the boundary layer. The overshoot in total temperature resembles that previously observed at wall temperature ratios close to unity and is attributed to viscous dissipation. Note that in the present investigation these effects persist to much lower wall temperatures and cause some perturbation of the profile for values of T_w/T_{o_e} as low as 0.535.

In the present tests most of the boundary layer is hypersonic. Assuming locally isentropic flow for the probe measurements, one may obtain the energy relationship

$$\left(\frac{u}{u_e}\right)^2 = \frac{M^2[1+(\gamma-1/2)M_e^2]}{M_e^2[1+(\gamma-1/2)M^2]}\frac{T_o}{T_{o_e}}$$

The hypersonic approximation ($M \gg 1$) to this relationship gives

$$(u/u_e)^2 \approx T_o/T_{o_e}$$

from this approximation

$$\frac{T_o - T_w}{T_{o_e} - T_w} = \frac{(u/u_e)^2 - T_w/T_{o_e}}{1 - T_w/T_{o_e}}$$

This apparently is the same equation used by Softley and Sullivan[21] to obtain their hypersonic limit.

Examination of this equation hereafter referred to as the hypersonic approximation reveals that as T_w/T_{o_e} approaches zero the functional relationship between $(T_o - T_w)/(T_{o_e} - T_w)$ and u/u_e for the hypersonic portion of the boundary layer approaches the quadratic relationship recently noted by a number of investigators. However, if T_w/T_{o_e} is greater than zero the value of the temperature relationship will fall below the quadratic. Thus, it

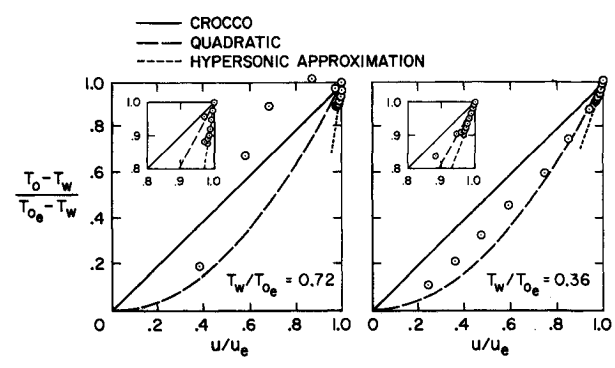

Fig. 7 Variations in velocity-temperature profiles with wall temperature ratio; $M_e \approx 27$, sta = 1.067 m.

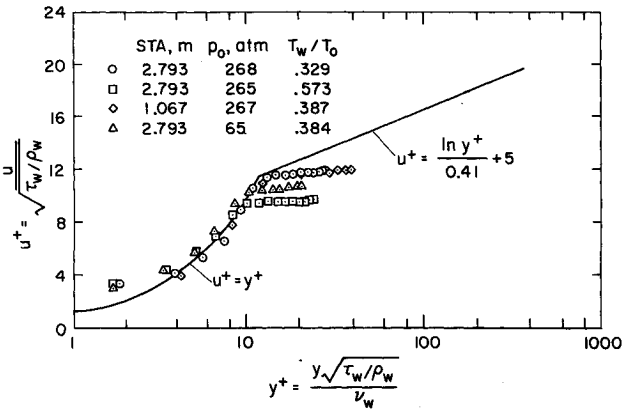

Fig. 8 Correlation of present velocity measurements using wall values.

appears that as edge Mach number increases, conditions may be encountered in the outer region of the boundary layer for flows on all types of bodies where the temperature-velocity relationship could vary substantially from the familiar Crocco relationship. Consequently, the deviation from a Crocco velocity-temperature relationship which has been observed recently may not be strictly a nozzle wall phenomenon as has been suggested,[19,20] but simply may be more evident in nozzle flows where the edge Mach number is generally higher, and where possible history effects coupled with pressure gradients tend to augment the differences. Softley and Sullivan[21] obtained data on a cone at $M = 10.2$ which agree very well with the hypersonic approximation. Furthermore the existence of hypersonic effects may explain why Jones and Feller's data[20] show very little tendency to "relax" to the linear profile for as much as 100 boundary-layer thicknesses downstream a nozzle exit.

Representative plots of the temperature-velocity relationship for the present tests are shown in Fig. 7. Excellent agreement occurs between the data and the hypersonic approximation in the outer region of the boundary layer. Although this region appears small, on this type of plot the hypersonic data cover about 75% of the boundary-layer thickness. In the viscous sublayer region the temperature-velocity relationship shows marked differences for the two temperature ratios presented in Fig. 7. The relationship for the higher wall temperature ratio is very complex as a result of the temperature overshoot in the sublayer. The lower wall temperature data show a much simpler behavior. However, in either case the temperature-velocity relationship is more complex than either the Crocco or the quadratic relationships indicate.

Correlations of the Velocity Profile

A correlation of the velocity profile using measured wall density and shear stress in law-of-the-wall parameters is presented in Fig. 8. The four cases shown represent considerable ranges in tunnel pressure, temperature, and station. In the viscous

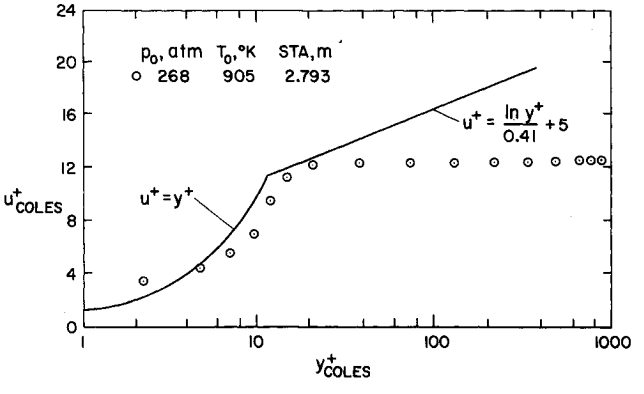

Fig. 9 Correlation of present velocity measurements using Cole's transformation.

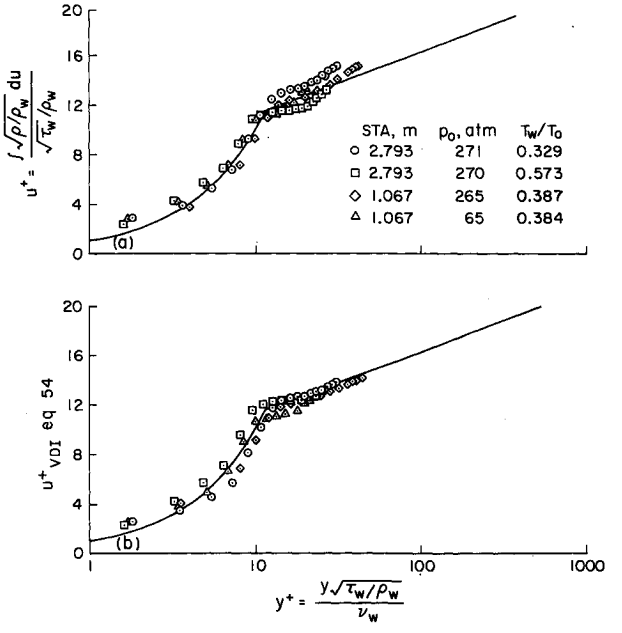

Fig. 10 Correlation of present velocity measurements using Van Driest transformation.

sublayer the data are in excellent agreement with incompressible correlation values,[22] however in the logarithmic region, the data do not agree with the incompressible correlation. In this region pressure and station affect the thickness of the turbulent region with increasing pressures causing increased thickness. On the other hand, changes in total temperature produce substantial effects on the relative level of $u/(\tau_w/\rho_w)^{1/2}$. Similar trends have also been observed in the data of Ref. 2.

Correlations of the present data using Coles'[23] and Van Driest's[24] transformations are shown in Figs. 9 and 10. Coles' transformation stretches the y variable using a function of the density variation across the boundary layer, As can be seen, with this transformation, the data retain the approximate agreement with the incompressible profile in the viscous sublayer while in the logarithmic region the y variable is stretched to values comparable to those obtained in incompressible flows. Although this transformation seems to stretch the y^+ variable to proper proportions it does not provide the changes in slope in the logarithmic region of the boundary layer that is required to provide complete agreement with incompressible data. It appears that the need for a slope change requires an operation on the velocity variable. Consequently, it is doubtful that other transformations which operate only on the y variable[25-27] will be successful in transforming the hypersonic turbulent boundary layer to the incompressible plane. On the other hand, the transformation of Van Driest's,[24] which operates only on the u variable, appears to successfully obtain a consistent correlation of the data as shown in Fig. 10. This figure shows two ways of applying the Van Driest transformation. The first uses the actual density profile to compute u^+ while the second uses Eq. (54) from Ref. 24 to compute u^+. This equation was obtained assuming a Crocco temperature velocity relationship. As indicated previously the Crocco relationship is somewhat different than the measured temperature velocity relationship. Therefore the substantial agreement of both curves indicates that, at least for the present test conditions, this transformation is not strongly affected by the assumed temperature-velocity relationship. Since the transformation operates only on u, the data terminate at the lower y^+ values. However, in other respects this transformation provides agreement between the present data and incompressible data.

Skin-Friction Measurement

The skin friction coefficient C_f is plotted vs R_θ in Fig. 11. Also shown in this figure are slopes for $C_f \propto R_\theta$, the familiar

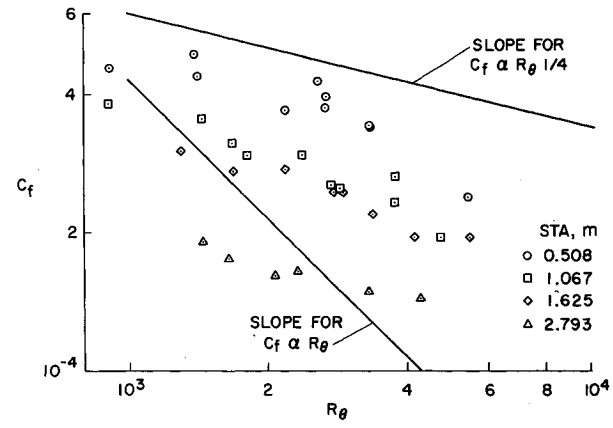

Fig. 11 Variations in C_f with R_θ.

relationship for laminar flow and $C_f \propto R_\theta^{1/4}$, the familiar relationship for turbulent flow. The data for any given station approximate the turbulent flow variation. However there are large differences between stations which primarily result from Mach number differences.

The present data are compared with three other sets of data[2,28,29] obtained on hypersonic nozzle walls and with five commonly used skin-friction prediction techniques[23,24,30-32] in Fig. 12. It appears that the tendency of most of the techniques to underpredict the friction at lower Mach numbers is amplified at the higher Mach numbers of the present tests. "Van Driest-I"[24] provides the best agreement with the data. This might be expected since it also provided a good transformation of the velocity profile data to the incompressible plane.

The existence of pressure gradient effects may introduce some disagreement between the data and the various predictions. However the present data and those of Fischer et al.[2] contains values obtained over a wide range of pressure gradients with no apparent differences attributable to this parameter.

Heat-Transfer Data

The heat-transfer coefficient C_H was computed using a recovery factor r of 0.8. This factor was obtained experimentally by fairing heat-transfer measurements near adiabatic wall conditions to determine the temperature for zero heat transfer. The value of r is lower than the 0.9 value previously measured in turbulent boundary layers at lower Mach number[33] and in fact is near the value for laminar boundary layers. The reasons for this are not understood, however it may result from the large thickness of the viscous sublayer dissipating turbulent bursts before they reach

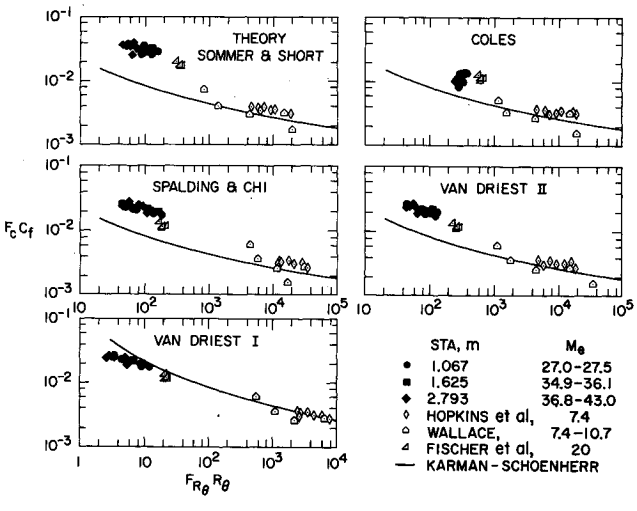

Fig. 12 Comparisons between measured and predicted skin friction.

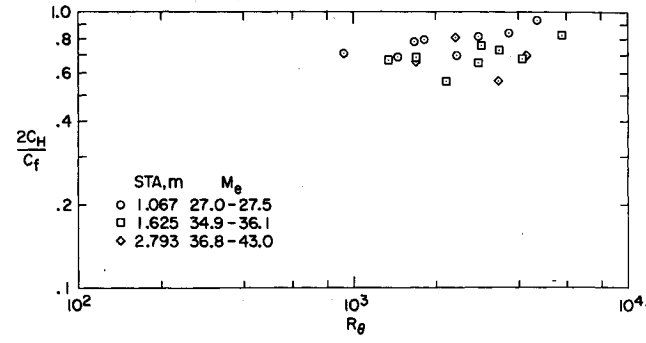

Fig. 13 Measured Reynolds analogy factors.

the wall. Comparisons of data have indicated that the temperature slope at the wall is consistent with the heat-transfer measurements. As was the case with skin friction, the heat transfer for any given station is closely approximated by the turbulent flow variation, $C_H \propto R_\theta^{1/4}$, with large differences between stations due to Mach number differences.

Reynolds analogy factors evaluated from measured skin friction and heat transfer are shown in Fig. 13. It is apparent that these Reynolds analogy factors are somewhat below those obtained in lower speed flows. The reasons for this are not fully understood at the present time. However there appears to be a tendency for the Reynolds analogy factor to increase with increasing Re_θ and decreasing Mach number.

Boundary-Layer Fluctuations

In Fig. 14 are shown oscilloscope traces indicating the fluctuations in heat transfer to the cooled film probe. Of interest here is the existence of the familiar intermittency at both the outer edge of the boundary layer and at the edge of the viscous sublayer. The inner intermittency resembles that reported by Corrsin et al[34] in incompressible flow and is as predominant as that at the outer edge of the boundary layer. Apparently turbulence dissipates in the viscous sublayer and it appears unlikely that large fluctuations ever reach the wall, probably as a result of the extreme thickness of the sublayer in the present case which results primarily from the very low density of the flow.

To demonstrate the effect of density on the thickness of these regions one can take y^+ from the correlations in Figs. 8 and 10 and the definition for shear stress, $\tau_w = \mu_w(\partial u/\partial y)_w \approx \mu_w(u_L/\delta_L)$, and arrive at the following relation for the laminar sublayer thickness

$$\delta_L = (\mu_w/\rho_w u_L)\,\text{const}$$

with the additional assumption $u_L \approx u_e$ (an assumption which

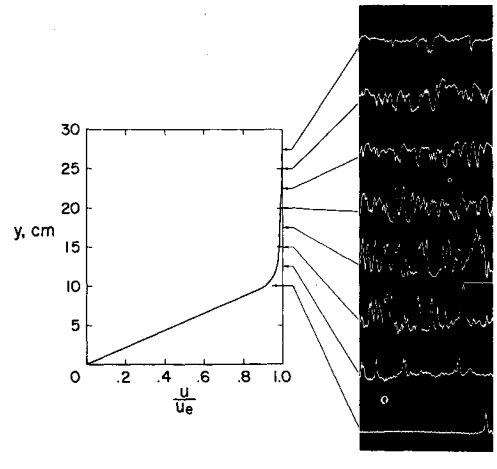

Fig. 14 Profile of heat transfer fluctuations to the cooled film probe; sta = 3.56 m, $M = 43.8$, $P_o = 201$ atm, $T_o = 538$.

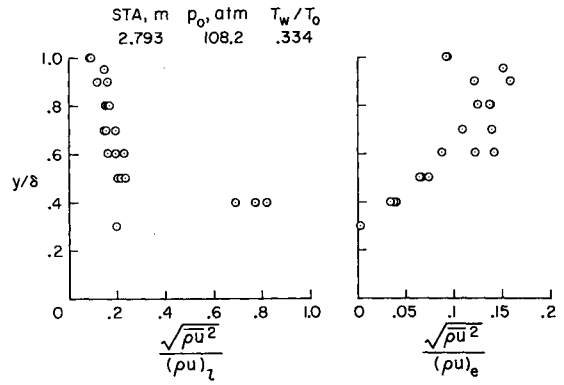

Fig. 15 Mass flow fluctuations through the boundary layer.

gives only a first-order approximation but appears to be more accurate at higher Mach numbers) one obtains

$$\delta_L = (\mu_w/\rho_w u_e)\text{const}$$

It becomes apparent that for constant u_e and T_w, δ_L is primarily affected by the density and may become very large if the density is sufficiently low. Furthermore, in constant pressure flows the viscous sublayer will be of nearly constant thickness.

The magnitude of the mass flow fluctuations are shown in Fig. 15. The first part of Fig. 15, where the mass flow fluctuations are normalized by local mean mass flow, shows a variation similar to that reported in Ref. 2. Here very large amplitude fluctuations on the order of 80% are observed near the edge of the viscous sublayer. This type of plot leaves one with the false impression that fluctuation amplitude increases with an approach to the edge of the sublayer when in fact the amplitude decreases as shown in the second part of Fig. 15 which uses the edge value of mass flow as the normalizing factor. Thus it appears that the main reason for the large relative amplitude of fluctuations is that the decrease in fluctuation amplitude lags the decrease in mean mass flow near the edge of the viscous sublayer.

The temperature fluctuations were nearly constant over the outer 70% of the boundary layer at a value between 1% and 2% probably as a result of the very low temperature gradient throughout most of the turbulent region.

The results presently available suggest as a possible flow model for hypersonic turbulent boundary layers that presented in Fig. 16. The regions shown here are essentially the same as those known to exist from previous investigations except for the intermittent region near the outer edge of the viscous sublayer. The basic difference between this model and those at lower Mach numbers is the relative extent of each region. It is probable that at high Mach numbers breakdown to turbulence originates in the outer region of the boundary layer[35-36] and that the low Mach angles associated with the very high Mach numbers restrict the region in which turbulence propagates. Thus it is likely that the rate of growth of the turbulent layer normal to the wall will be restricted. From this and the fact that low densities typically associated with high Mach number flows leads to very thick viscous sublayers, as mentioned above, it appears likely that there will be a substantial region of flow where the viscous sublayer is of the same order of thickness as the intermittent and turbulent

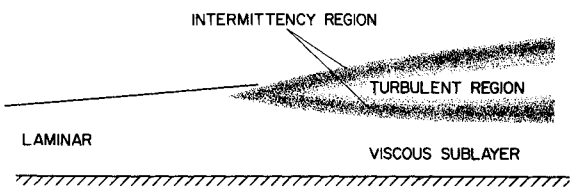

Fig. 16 Schematic drawing of a proposed hypersonic turbulent boundary-layer flow model.

regions. Another equally important feature which may have far-reaching consequences is that the very thick sublayer seems to provide a cushioning which reduces the effect of turbulence on the wall. This is evident in the apparent dissipation of the turbulence near the wall which may account for the very small differences between laminar and turbulent skin friction at high Mach numbers and the existence of relatively lower heat-transfer rates than are normally expected for turbulent flow.

Conclusions

Extensive measurements on the wall and across the turbulent boundary layer of a very high Mach number nozzle indicate: 1) Temperature profiles are more complex than the Crocco or quadratic relationships observed previously at lower Mach numbers. 2) Van Driest's transformation of the velocity profiles provides reasonable agreement with incompressible data. 3) Both recovery factor and Reynolds analogy factor have somewhat lower values than these observed in lower Mach number tests. 4) An intermittent region exists not only at the outer edge of the boundary layer, but also at the outer edge of the viscous sublayer.

Appendix: Derivation of Parameters Used to Correlate Total-Temperature-Probe Calibration Data

If it is assumed that radiation losses are the major source of error, and that the conduction losses can be neglected, then the relationship for determining recover factor of the probe is

$$r = f(h/T_o^4)$$

where

$$h = (k/D)N_{u_w}$$

Furthermore, since the wire diameter is very small and the densities very low, it is reasonable to assume that the Nusselt number variation may be approximated by the free molecular value

$$N_{u_w} \propto Re_w$$

For helium

$$Re_w \approx \rho_w T_o^{-0.147} D$$

and

$$k \propto T_o^{0.647}$$

thus

$$h/T_o^4 \propto \rho_w/T_o^{3.5} \propto P_2/T_o^{4.5}$$

or

$$r = f(P_2/T_o^{4.5})$$

References

[1] Kemp, J. H., Jr. and Sreekanth, A. K., "Preliminary Results from an Experimental Investigation of Nozzle Wall Boundary Layers at Mach Numbers Ranging from 27 to 47," AIAA Paper 69-686, San Francisco, Calif., 1969.

[2] Fischer, M. C., Maddalon, D. V., Weinstein, L. M., and Wagner, R. D., Jr., "Boundary-Layer Surveys on a Nozzle Wall at $M_\infty \approx 20$ Including Hot-Wire Fluctuation Measurements," *AIAA Journal*, Vol. 9, No. 5, May 1971, pp. 826–834.

[3] Kemp, J. H., Jr., "The Ames M-50 Helium Tunnel," TN D-5788, 1970, NASA.

[4] Thurtell, G. W. and Tanner, C. B., "Momentum Transport Measurement in the Atmospheric Surface Layer With the Anemoclinometer," Final Rept. 1962–65, 1965, Dept. of Soil Science, Univ. of Wisconsin, Madison, Wis.

[5] Arney, G. D., Jr. and Bailey, A. B., "An Investigation of the Equilibrium Pressure Along Unequally Heated Tubes," AEDC-TDR-62-26, Feb. 1962, Arnold Engineering Development Center, Tullahoma, Tenn.

[6] Arney, G. D., Jr. and Bailey, A. B., "Addendum to an Investigation of Equilibrium Pressures Along Unequally Heated Tubes," AEDC-

TDR-62-188, Oct. 1962, Arnold Engineering Development Center, Tullahoma, Tenn.

[7] Potter, J. L., Kinslow, M., and Boylan, D. E., "An Influence of the Orifice on Measured Pressures in Rarefied Flow," AEDC-TDR-64-175, Sept. 1964, Arnold Engineering Development Center, Tullahoma, Tenn.

[8] Potter, J. L. and Bailey, A. B., "Pressures in the Stagnation Regions of Blunt Bodies in the Viscous-Layer to Merged-Layer Regimes of Rarefied Flow," AEDC-TDR-63-168, Sept. 1963, Arnold Engineering Development Center, Tullahoma, Tenn.

[9] Horstman, C. C., "Surface Pressures and Shock-Wave Shapes on Sharp Plates and Wedges in Low Density Hypersonic Flow," *Proceedings of 6th International Symposium on Rarefied Gas Dynamics*, Vol. 1, Academic Press, New York, 1969, pp. 593–605.

[10] Winkler, E. M., "Stagnation Temperature Probes for Use at High Supersonic Speeds and Elevated Temperatures," NAVORD Rept. 3834, Oct. 1954,

[11] Spangler, J. D., "A Sensitive Magnetic Balance for the Direct Measurement of Skin Friction Drag," LTV Rept. 0-71000/3R-29, Dec. 1963,

[12] Coles, D., "Measurements in the Boundary Layer on a Smooth Flat Plate in Supersonic Flow," Ph.D. thesis, 1953, Calif. Inst. of Tech., Pasadena, Calif.

[13] Dhawan, S., "Direct Measurements of Skin Friction," TR-1121, 1953, NACA.

[14] Fenter, F. W., "Analyses and Direct Measurement of the Skin Friction of Uniformly Rough Surfaces at Supersonic Speeds," IAS Preprint 837, July 1958, Institute of Aeronautical Sciences.

[15] McCroskey, W. J., "An Experimental Model for the Sharp Leading Edge Problem in Rarefied Hypersonic Flow," Ph.D. thesis, Jan. 1966, Princeton Univ., Princeton, N.J.

[16] Kistler, A. L., "Fluctuation Measurements in a Supersonic Turbulent Boundary Layer," *Physics of Fluids*, Vol. 2, No. 3, May-June 1959, pp. 290–296.

[17] Bach, L. H., Massier, P. F., and Cuffel, R. F., "Some Observations on the Reduction of Turbulent Boundary Layer Heat Transfer in Nozzles," *AIAA Journal*, Vol. 4, No. 12, Dec. 1966, pp. 2226–2229.

[18] Bach, L. H., Cuffel, R. F., and Massier, P. F., "Laminarization of a Turbulent Boundary Layer in Nozzle Flow," *AIAA Journal*, Vol. 7, No. 4, April 1969, pp. 730–733.

[19] Bushnell, D. M., Johnson, C. B., Harvey, W. D., and Feller, W. V., "Comparison of Prediction Methods and Studies of Relaxation in Hypersonic Turbulent Boundary Layers," NASA SP 216, 1969, pp. 345–376.

[20] Jones, R. A. and Feller, W. V., "Preliminary Surveys of the Wall Boundary Layer in a Mach 6 Axisymmetric Tunnel," TN D-5620, 1970, NASA.

[21] Softley, E. J. and Sullivan, R. J., "Theory and Experiment for the Structure of Some Hypersonic Boundary Layers," AGARD-CP-30, May 1968, pp. 3-1–3-18.

[22] Coles, D., "Measurements in the Boundary Layer on a Smooth Flat Plate in Hypersonic Flow. III Measurements in a Flat Plate Boundary Layer at the Jet Propulsion Laboratory," JPL Rept. 20-71, 1953, Jet Propulsion Lab., Pasadena, Calif.

[23] Coles, D., "The Turbulent Boundary Layer in a Compressible Fluid," *Physics of Fluids*, Vol. 7, No. 9, Sept. 1964, pp. 1403–1423.

[24] Van Driest, E. R., "Turbulent Boundary Layers in Compressible Fluid," *Journal of the Aerospace Sciences*, Vol. 18, No. 3, March 1951, pp. 145–160, 216.

[25] Mager, A., "Transformation of the Compressible Turbulent Boundary Layer," *Journal of the Aerospace Sciences*, Vol. 25, No. 5, May 1958, pp. 305–311.

[26] Baronte, P. O. and Libby, P. A., "Velocity Profile in Turbulent Compressible Boundary Layers," *AIAA Journal*, Vol. 4, No. 2, Feb. 1966, pp. 193–202.

[27] Laufer, J., "Turbulent Shear Flows of Variable Density," *AIAA Journal*, Vol. 7, No. 4, April 1969, pp. 706–713.

[28] Wallace, J. E., "Hypersonic Turbulent Boundary-Layer Measurements Using an Electron Beam," Final Rept., Oct. 1966-May 1968, NASA SP 216, 1968, pp. 255–308; also CAL Rept. AN-2112-1, Aug. 1968, Cornell Aeronautical Lab.,

[29] Hopkins, E. J., Rubesin, M. W., Inouye, M., Keener, E., Mateer, G., and Polek, T. E., "Summary and Correlation of Skin Friction and Heat Transfer Data for a Hypersonic Turbulent Boundary Layer on Simple Shapes," NASA SP 216, 1969, pp. 319–344.

[30] Sommer, S. C. and Short, B. J., "Free-Flight Measurements of Skin Friction of Turbulent Boundary Layers with High Rates of Heat Transfer at High Supersonic Speeds," TN 3391, 1955, NACA, also *Journal of the Aeronautical Sciences*, Vol. 23, No. 6, June 1956, pp. 536–542.

[31] Spalding, D. B. and Chi, S. W., "The Drag of a Compressible Turbulent Boundary Layer on a Smooth Flat Plate With and Without Heat Transfer," *Journal of Fluid Mechanics*, Vol. 18, Pt. 1, Jan. 1964, pp. 117–143.

[32] Van Driest, E. R., "Problem of Aerodynamic Heating," Aero Aspects Session, Nat'l Summer Meeting IAS, Los Angeles, 1956; also *Aeronautical Engineering Review*, Vol. 15, No. 10, Oct. 1956, pp. 26–41.

[33] Rudy, D. H. and Weinstein, L. M., "Investigation of Turbulent Recovery Factor in Hypersonic Flow," *AIAA Journal*, Vol. 8, No. 12, Dec. 1970, pp. 2286–2287.

[34] Corrsin, S., "Some Current Problems in Turbulent Shear Flow," *Proceedings First Symposium Naval Hydrology*, National Academy of Science, Johns Hopkins Univ., 1951.

[35] Nagamatsu, H. T., Braber, B. D., and Sheer, R. E., "Critical Layer Concept Relative to Hypersonic Boundary Layer Stability," GE Rept. 66-C-192, 1966, General Electric Co.,

[36] Maddalon, D. V. and Henderson, A., Jr., "Boundary-Layer Transition on Sharp Cones at Hypersonic Mach Numbers," *AIAA Journal*, Vol. 6, No. 3, March 1968, pp. 424–431.